Effect of Longitudinal Reinforcements in Reinforced Concrete Piers Subjected to Blast Loading

Aswin Vijay, K Subha

Abstract— The increase in the world population day by day demands an equivalent increase in infrastructure. Viaducts contribute to a major portion of the infrastructure. Majority of these viaducts rests on reinforced concrete piers. Accidental or intentional blasts can damage the pier structures resulting in loss of life and property. The journal is regarding the effects of the longitudinal bars of these reinforced concrete piers in resisting the deformation caused by blast loads and the stresses developed during the same.

Index Terms— Blast, Explosion, Blast Waves, Blast loading, Reinforcement, Concrete Piers, Viaduct, Explosive Effects, Blast Loading.

1 Introduction

THE increase in population over the years have led to a rapid increase in the infrastructure. The same has also led to an increase in the number of accidents and acts of vandalism over the years. As a result, blasts, accidental as well as intensional, are happening all over the world. A major portion of the infrastructure are viaducts. Many of them are elevated and rests on reinforced concrete piers. These piers generally do not have any protection except for a small crash barrier. The failure of these pier structures can cause the structure to fail and topple over. In modern metros, roads are running on either side of these piers, as the metros are constructed above roads. Any accident involving a blast can damage or destroy the pier structures, resulting in serious damage and loss of life. Designing the piers to be blast resistant can help in minimizing the casualties. By studying about the loads generated and their action on the pier structure, we can design the piers to withstand blast loads. But, designing the structure to resist the blast completely will be uneconomical. Thus, it is advisable to find a balance between safety and economy. As science is evolving, chemicals used for explosions are also evolving. Many modern chemical explosives cannot be traced even by using the state of the art detection devices and techniques. So, it is better that we stay prepared to face such a scenario.

2 Analysis Concepts

2.1 Explosion and Blast

An explosion is a rapid increase in volume and release of energy in an extreme manner, usually accompanied with the generation of high temperatures and the release of gases. Supersonic explosions created by high explosives are known as detonations and travel as supersonic waves. Subsonic explosions are created by low explosives through a slower burning process known as deflagration. When caused by a man-made device such as an exploding rocket or firework, the audible component of an explosion is referred to as its report.

Blast is the pressure disturbance caused by the sudden release of energy. Blast pressure is more properly overpressure, because it is relative to ambient conditions, rather than absolute pressure. Shock waves are high pressure waves that travel through air (or other medium) at a velocity faster than the speed of sound. Shockwaves are characterized by an instantaneous increase in pressure followed by a rapid decay. Pressure waves have lower amplitude and travel below the speed of sound. Pressure waves are characterized by a more gradual increase in pressure than a shock wave, with a decay of pressure much slower than shock wave. In most cases, shock waves have a greater potential for damage and injury than pressure wave.

As a blast wave travels away from the source, the pressure amplitude decreases, and the duration of blast load increases. Overexpansion at the center of the blast creates a vacuum in the source region and a reversal of gas motion. This negative pressure region expands outwards causing a negative phase (below ambient), which trails the positive phase value. The negative phase pressure is generally lower in magnitude (absolute value) but longer in duration than the positive phase. Generally speaking, positive phase blast loads are more consequential than negative phase load, later of which is often ignored.

Expansion of the blast wave causes air particles to move outward during the positive phase and inward during the negative phase. The flow of air particles creates a pressure analogous to that caused by wind. The pressure produced by this flow is referred to as dynamic pressure. This pressure is lower in magnitude than the shock or pressure wave and imparts a drag load similar to wind loads on objects in its path.

As the shock wave strikes a wall or other object, a reflection occurs, increasing the applied pressure on the surface. This reflected pressure is considerably higher than the incident pressure wave. At the free edges of a reflection surface, the discontinuity between the forward travelling incident blast

- *Author Aswin Vijay is currently pursuing masters degree program in structural engineering in APJ Abdul Kalam Technological University, Kerala, India, PH- +918547215625. E-mail: me.aswinvijay@gmail.com*
- *Co-Author K Subha is currently working as the Head of Department of Civil Engineering, NSS College of Engineering, Palakkad under the APJ Abdul Kalam Technological University, Kerala, India. E-mail: subha.kasthuril@gmail.com*

wave and rearward travelling reflected blast wave creates a rarefaction, or pressure relief wave. Rarefactions travel inward from the outer edges across the face of the reflection surface. The rarefaction waves relieve the positive reflected pressure down to the free-field or side-on pressure, plus drag pressure. The peak reflected pressure is not affected, only the duration. The time required for the rarefaction waves to completely relieve the reflected pressure is termed the clearing time. This clearing time varies across the surface. It should be noted that a rarefaction wave does not instantaneously clear reflected pressure; rather, the relief is somewhat gradual and takes longer than the time required for the leading edge of the rarefaction to travel to the center of the reflected surface. If the clearing time exceeds the positive phase blast wave duration, clearing does not affect the positive phase loads.

2.2 Sources of Blast

Expansion of the blast wave causes air particles to move outward during the positive phase and inward during the negative phase. The flow of air particles creates a pressure analogous to that caused by wind. The pressure produced by this flow is referred to as the dynamic pressure. This pressure is lower in magnitude than the shock or pressure wave and imparts a drag load similar to wind loads on objects in its path.

Blasts involving chemical reactions can be classified by their reaction rates into two primary groups: deflagration and detonations. A deflagration is an oxidation reaction that propagates at a rate less than the speed of sound in the unreacted material. The corresponding blast wave is often termed a pressure wave and has a finite rise time, as illustrated in Fig.1. A fast deflagration can create a more sudden rise in pressure. By contrast, in a detonation, the reaction front propagates supersonically, usually many times faster than the speed of sound. This blast wave is termed a shock wave and has an instantaneous rise in pressure, as seen in Fig.2. Since pressure is closely related to reaction rate, detonation pressures are usually many times higher than deflagration pressures.

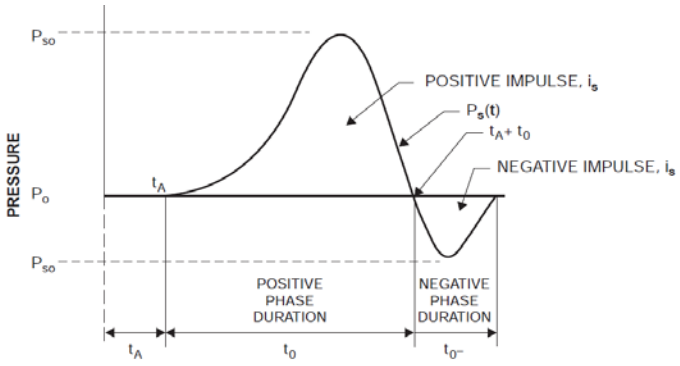

Fig.1 Pressure Wave from Deflagration

Deflagration and detonations may involve oxidizers and fuels that are oxygen-deficient or materials that may produce flammable gases as a product of reaction. In either case, the unreacted or flammable products may mix with air and result in secondary burning. The secondary burning does not contribute significantly to the blast pressures for external explosions but can be a major consideration for predicting internal explosion blast pressures.

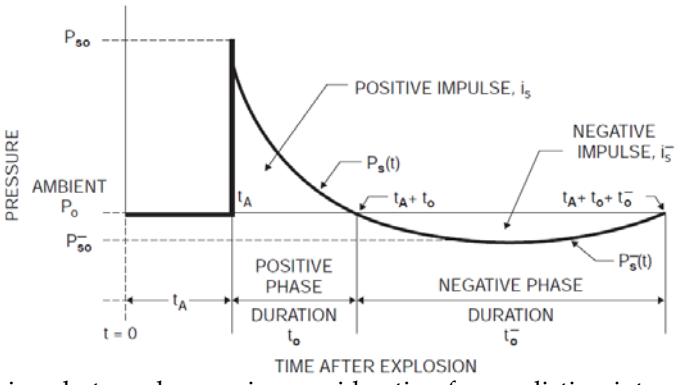

Fig.2 Shock Wave from Detonation

2.3 Types of Blast

There are 3 kinds of explosions which are unconfined explosions, confined explosions and explosions caused by explosives attached to the structure.

Unconfined explosions can occur as an air-burst or a surface burst. In an air burst explosion, the detonation of the high explosive occurs above the ground level and intermediate amplification of the wave caused by ground reflections occurs prior to the arrival of the initial blast wave at a building (Fig.3) As the shock wave continues to propagate outwards along the ground surface, a front commonly called a Mach stem is formed by the interaction of the initial wave and the reflected wave.

However, a surface burst explosion occurs when the detonation occurs close to or on the ground surface. The initial shock wave is reflected and amplified by the ground surface to produce a reflected wave. (Fig.4) Unlike the air burst, the reflected wave merges with the incident wave at the point of detonation and forms a single wave. In the majority of cases, terrorist activity occurs in built-up areas of cities, where devices are placed on or very near the ground surface.

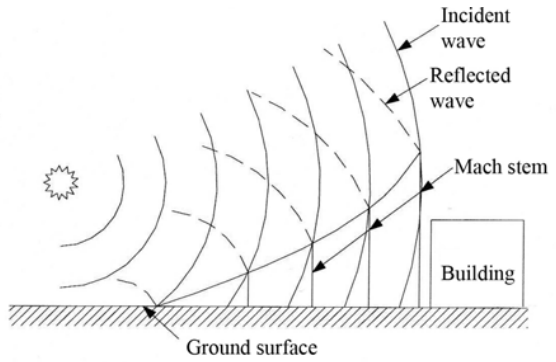

Fig.3 Air Burst with Ground Reflections

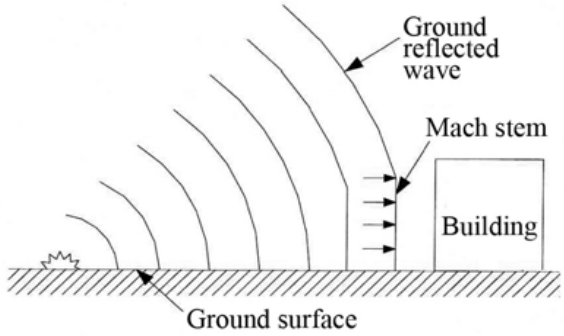

Fig.4 Surface Burst

An explosion occurs when a gas, liquid or solid material goes through a rapid chemical reaction. When the explosion occurs, gas products of the reaction are formed at a very high temperature and pressure at the source. These high-pressure gases expand rapidly into the surrounding area and a blast wave is formed. Because the gases are moving, they cause the surrounding air move as well. The damage caused by explosions is produced by the passage of compressed air in the blast wave. Blast waves propagate at supersonic speeds and reflected as they meet objects. As the blast wave continues to expand away from the source of the explosion its intensity diminishes and its effect on the objects is also reduced.

Close to the source of explosion the blast wave is formed and violently hot and expanding gases will exert intense loads which are difficult to quantify precisely. Once the blast wave has formed and propagating away from the source, it is convenient to separate out the different types of loading experienced by the surrounding objects. Three effects have been identified in three categories. The effect rapidly compressing the surrounding air is called "air shock wave". The air pressure and air movement effect due to the accumulation of gases from the explosion chemical reactions is called "dynamic pressure" and the effect rapidly compressing the ground is called "ground shock wave".

The air shock wave produces an instantaneous increase in pressure above the ambient atmospheric pressure at a point some distance from the source. This is commonly referred to as overpressure. As a consequence, a pressure differential is generated between the combustion gases and the atmosphere, causing a reversal in the direction of flow, back towards the center of the explosion, known as a negative pressure phase. This is a negative pressure relative to atmospheric, rather than absolute negative pressure. (Fig.5). Equilibrium is reached when the air is returned to its original state.

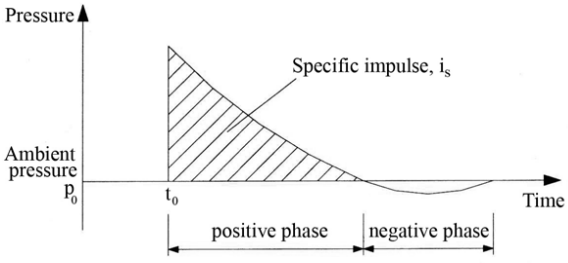

Fig.5 Blast Wave Pressures Plotted Against Time

As a rough approximation, 1kg of explosive produces about one m^3 of gas. As this gas expands, its act on the air surrounding the source of the explosion causes it to move and increase in pressure. The movement of the displaced air may affect nearby objects and cause damage. Except for a confinement case, the effects of the dynamic pressure diminish rapidly with distance from source.

The ground shock leaving the site of an explosion consists of three principal components. A compression wave which travels radially from the source; a shear wave which travels radially and comprises particle movements in a plane normal to the radial direction where the ground shock wave intersects with the surface and a surface or Raleigh wave. These waves propagate at different velocities and alternate at different frequencies.

2.4 Characteristics of Blast Wave

Fig.6 shows a comparison between free-field or side on, and reflected pressure - time histories. The parameters shown in these figures are defined as:

P_o = Ambient pressure
P_{so} = Peak positive side-on overpressure
P_{so-} = Peak negative side-on overpressure
$P_{s(t)}$ = Time varying positive overpressure
$P_{s(t)-}$ = Time varying negative overpressure
P_r = Peak reflected overpressure
I_s = Positive-phase-specific impulse, the integration of the positive phase pressure-time history
I_{s-} = Negative-phase-specific impulse, the integration of the negative phase pressure-time history
t_a = Time of arrival
t_o = Positive phase duration
t_{o-} = Negative phase duration

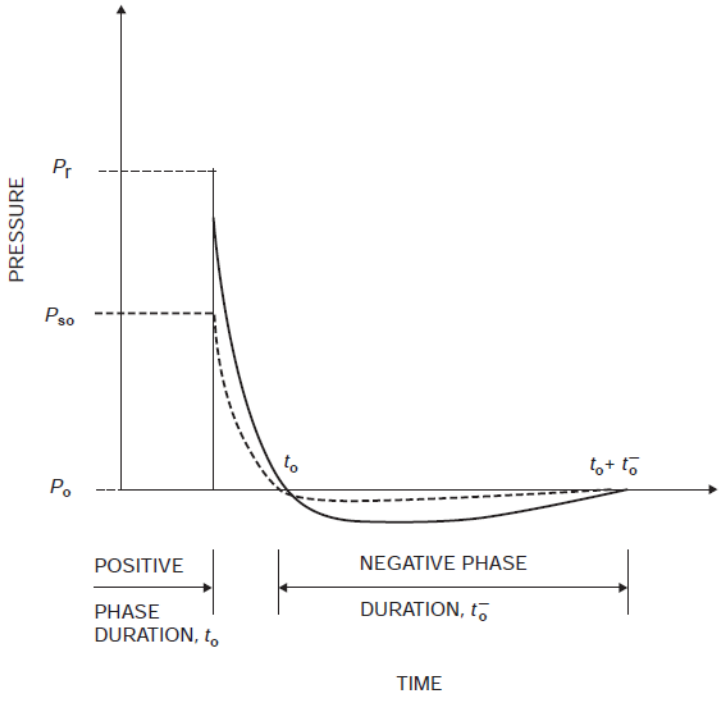

Fig.6 Comparison of Free Field and Reflected Blast Loads

The term "overpressure" refers to a gauge pressure, or the

blast pressure relative to ambient pressure. Free-field loads are those produced by blast waves sweeping over surfaces unimpeded by any objects in their path. This load is also referred to as side - on when the blast wave sweeps over a wall or other object parallel to its direction of travel. Side-on pressure terms are indicated by a "so" subscript in the Fig.6.

2.5 Prediction of Blast Parameters

Predicting blast loads for various explosives can be challenging. There is much less data available for propellants and pyrotechnics than for high explosives, with respect to blast loads. Burn rates, gas generation, and energy output rate values can be used to perform a burn simulation and determine the gas pressure load in a confined area. In some cases, TNT equivalencies for these materials have been used. However, this is problematic because peak pressure for propellants and pyrotechnics is much lower than for TNT, but the impulse of propellants can be higher in a confine space than for the TNT equivalent. Care must be taken when equivalencies are based on small-scale tests, as large quantities may react in a more energetic manner.

The methods available for prediction of blast effects on buildings structures are empirical methods, semi-empirical methods and numerical methods. Empirical methods are essentially correlations with experimental data. Most of these approaches are limited by the extent of the underlying experimental database. The accuracy of all empirical equations diminishes as the explosive event becomes increasingly near field. Semi-empirical methods are based on simplified models of physical phenomena. The attempt is to model the underlying important physical processes in a simplified way. These methods are dependent on extensive data and case study. The predictive accuracy is generally better than that provided by the empirical methods. Numerical (or first-principle) methods are based on mathematical equations that describe the basic laws of physics governing a problem. These principles include conservation of mass, momentum, and energy. In addition, the physical behavior of materials is described by constitutive relationships. These models are commonly termed computational fluid dynamics (CFD) models.

There are various relationships and approaches for determining the incident pressure value at a specific distance from an explosion. All the proposed relationships entail computation of the scaled distance, which depends on the explosive mass and the actual distance from the center of the spherical explosion.

Some common theories adopted for the computation of blast parameters are Brode's theory, Newmark's Theory, Mill's theory etc. However, for this particular work, Brode's theory was selected.

2.6 Brode's Theory

The calculation of blast load is a tedious process. In this work, only blasts generated by spherical charges is considered. Spherical charges imply that the energy generated during the explosion propagates in all directions. This happens when the explosions take place above the ground surface. Only unconfined explosions taking place above the ground surface is considered. The blast pressures generated due to these charges are calculated using Brode's theory. According to Brode's theory, the peak overpressure for spherical blast depend on the magnitude of the explosion. Equation 1 is valid where the peak overpressure is over 10 bars (=1MPa) (near field explosions) and Equation 2 for pressure values between 0.1 bar and 10 bars (0.01MPa-1MPa) (medium and far-field explosions). The scaled distance is measured in m/kg^3 and the pressure Pso in bars,

$$P_{so} = (6.7/Z^3) + 1 \text{ , for Pso} > 10 \text{ bars} - \{\text{Equation 1}\}$$

$$P_{so} = (0.975/Z) + (1.455/Z^2) + (5.85/Z^3) - 0.019, \text{ for } 0.1 < \text{Pso} < 10 \text{ bars} - \{\text{Equation 2}\}$$

$$\text{where, } Z = (R/W^{(1/3)}) \{\text{Equation 3}\}$$

R is the standoff distance in m and w is the charge weight expressed in kg as the equivalent weight of TNT.

3 Analysis

The analysis is done in two methods. First one, by fixing the charge weight used for creating the explosion and the second one, by varying the standoff distance of the explosion. For this purpose, the charge weight is fixed as 250 kg of TNT. This is the maximum amount of TNT that can be transported using a small car. The standoff distance is varied between 5 m to 25 m to study the effects of standoff distance to the deformations and stresses generated in the structure.

In the second method, the standoff distance is kept fixed and the charge weight causing the explosion is varied. This helps in analyzing the effects of charge weight on the stresses and deformations generated. For this purpose, the standoff distance is adopted a 5 m. The value of 5 m is adopted because two lane roads are running on either side of the metro and 5 m is the distance at which a vehicle can be parked closest to the metro pier avoiding suspicion. The charge weight causing the explosion is varied between 250 kg to 1500 kg of TNT. 1500 kg amounts to the amount of TNT that can be transported in a medium sized truck.

The blast loads acting on the structure was calculated and all the cases are modeled in ANSYS and solved by the explicit dynamic solver using Autodyn. Loads are applied on the curved surface area of the circular piers having a diameter of 1.6 m and a height of 5.5 m exposed to the blast. Support conditions are assigned. The bottom of the pier has a fixed support condition while the top acts as a hinged support. M 40 and M 50 grades of concrete are considered in this work and the grade of steel is opted as Fe 415. The behavior between the contact region of steel and concrete is also specified. Earth gravity was also modelled.

The percentage reinforcement of 0.8% to 6% has been considered in the analysis. This range of percentage reinforcements was adopted for the analysis since 0.8% is the minimum and 6% is the maximum theoretical values of the percentage of steel to be provided in a column or a pier according to the Indian standards. The diameter of main bars is taken as 32 mm. Thus, while arranging the bars in the pier and considering the

clauses regarding the spacing of the reinforcement in a pier as per the Indian standards, upto 2.5% reinforcement satisfies the clauses. According to the Indian standards, the spacing between the bars should be greater than the diameter of the largest diameter bar used. Above 2.5% of reinforcement this is not satisfied. Thus, for analysis purpose, percentage reinforcements varying from 0.8% to 2.5% is considered. A clear cover of 40 mm is also provided to the piers according to the Indian standard codes.

The analysis is a done for three arrangements of the stirrups. Circular ties of Fe 415 bar of 8 mm diameter are provided as the stirrup. The stirrups are given at a spacing of 100 mm, 200 mm and 300 mm and all possible combinations for various steel percentages of steel are analyzed. Another set of models in which only the longitudinal reinforcements are present without any stirrups were also analyzed. This is done to set a benchmark for the comparison of analysis values obtained for the various stirrup arrangements.

Meshing was done automatically by the software. The longitudinal bars as well as the stirrups were assigned link elements and the concrete was assigned solid elements. In link elements only axial forces are considered. This is done to minimize the number of elements and to reduce the computation time.

While considering the analysis results, tensile stresses are considered to be critical for concrete, as the concrete is weak in tension. The value of tensile strength of concrete is very less compared to its compressive strength. The failure of concrete due to crushing was not obtained in any of the analysis cases. Thus, the stress values taken represents the tensile stresses developed in the concrete. The stress and deformation values are obtained from ANSYS.

4 Results

Analysis is conducted for various percentages of reinforcement. 0.8%, 1%, 1.5%, 2%, and 2.5% reinforcement was considered for this purpose. This is done for concretes of grade M 40 and M50. The analysis is also done by varying the location of blast, charge weight, spacing of the stirrups. All possible combinations were considered and analyzed. Various graphs are generated for the comparison and typical graphs are given below.

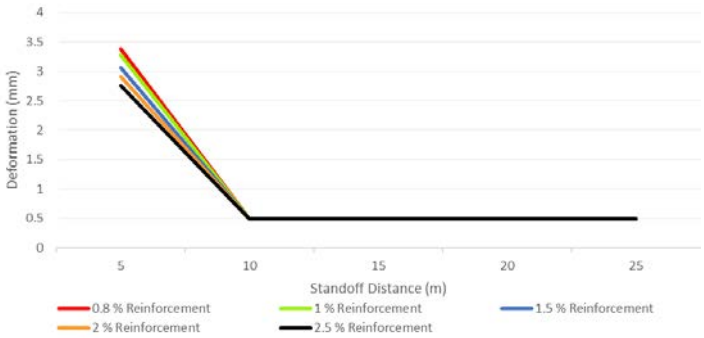

Fig.7 Standoff distance vs Deformation - M 40, 250 kg of TNT and Stirrups at 300 mm

Table.1. Standoff distance vs Deformation - M 40, 250 kg of TNT and Stirrups at 300 mm

Standoff Distance (m)	Maximum Deformation (mm) for reinforcement percentages				
	0.8 %	1 %	1.5 %	2 %	2.5 %
5 m	3.3782	3.2807	3.0618	2.9082	2.7639
10 m	0.49122	0.49122	0.49122	0.49122	0.49122
15 m	0.49123	0.49123	0.49123	0.49123	0.49123
20 m	0.49123	0.49123	0.49123	0.49123	0.49123
25 m	0.49123	0.49123	0.49123	0.49123	0.49123

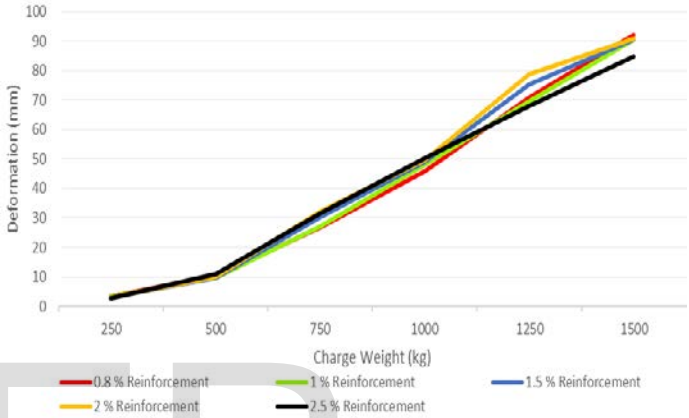

Fig.8 Charge Weight vs Deformation - M 40, 5 m Blast and Stirrups at 300 mm

Table.2. Standoff distance vs Deformation - M 40, 5 m Blast, Stirrups at 300 mm

Charge Weight (kg)	Maximum Deformation (mm) for reinforcement percentages				
	0.8 %	1 %	1.5 %	2 %	2.5 %
250 kg	3.3782	3.2807	3.0618	2.9082	2.7639
500 kg	10.186	9.8394	9.6067	9.9989	10.994
750 kg	26.944	27.246	30.146	32.156	31.603
1000 kg	45.753	47.92	48.917	49.567	50.346
1250 kg	70.927	69.745	75.396	78.895	68.146
1500 kg	92.251	90.698	90.662	90.819	84.911

Considering the deformation result, it can be seen that deformation is maximum for 0.8% reinforcement in all cases where the charge weight is fixed as 250 kg of TNT. However, in the cases where the standoff distance is fixed, the values of deformations is maximum for the pier with 0.8% reinforcement in case of M 40 concrete. For M 50 grade of concrete, this is not so. It can be observed that the values of deformations are maximum for piers with 2.5% reinforcement. The deformations of M 50 grade of concrete are less when compared to that of M 40 grade concrete for the similar cases.

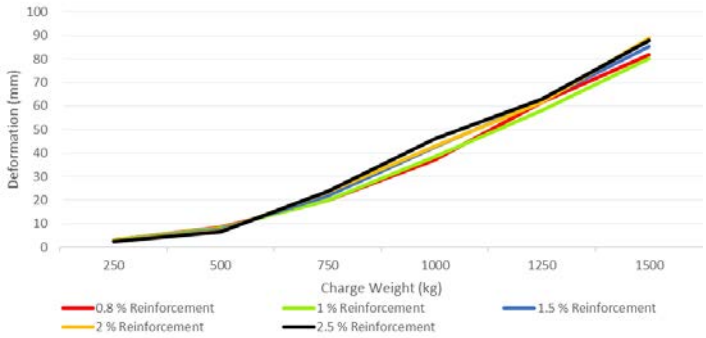

Fig.9. Charge Weight vs Deformation - M 50, 5 m Blast and Stirrups at 200 mm

Table.3. Standoff distance vs Deformation - M 50, 5 m Blast and Stirrups at 200 mm

Charge Weight (kg)	Maximum Deformation (mm) for reinforcement percentages				
	0.8 %	1 %	1.5 %	2 %	2.5 %
250 kg	3.0539	2.9762	2.7958	2.6685	2.5464
500 kg	8.6103	8.2447	7.5437	7.0723	6.7004
750 kg	20.002	19.857	21.775	23.402	23.807
1000 kg	37.302	38.516	42.541	42.976	46.128
1250 kg	61.798	58.242	62.203	61.836	63.03
1500 kg	81.737	80.269	85.31	88.654	87.967

For a charge weight of 250 kg, at a standoff distance of 5 m, the deflections produced are not very high. In fact, the deformations produced are within the permissible limits. Only small cracks will be developed on the outer surface of the pier. This case does not account to a structural damage that is to be rectified. As the standoff distance increases the deformation decreases to a particular value. Hence, irrespective of the standoff distance a small amount of deformation is generated in the pier for a standoff distance of 10 m and above. This deformation is most probably generated by the propagating air blast waves whose energy is dissipated along the path.

In the cases where the standoff distance is kept fixed at 5 m, and varying the charge weight used between 250 kg and 1500 kg of TNT, the deformations are within the permissible limits for charge weight in the range 600 kg to 700 kg of TNT depending on the percentage reinforcement of the pier. Over this range of charge weights, the piers deform by over 20 mm which is the limiting value of deformation as per the Indian standards. Thus, above this range, structural damage will be generated in the piers which must be rectified.

Considering the stresses obtained from the analysis, in cases where the charge weight is fixed, the stress developed is found to be highest in case of piers with 0.8% reinforcement and lowest in piers with 2.5% reinforcement. All the other cases of percentage reinforcement fall between these two. It is found that the stresses decrease as the standoff distance increases, possibly due to the energy dissipation along the path. In the cases where the standoff distance is kept constant, the variation of stresses is highly irregular. However, on a general note, it can be seen that the stresses are higher for piers with 0.8% reinforcement and less for piers with 2.5% reinforcements just like in the case of fixed charge weight. The stresses developed in the piers keeps on increasing as the charge weight causing explosion increases. For M 40 grade concrete, the maximum tensile stress the concrete can resist without developing cracks is 4.42 MPa, and for M 50 grade concrete, this value is 4.94 MPa as per Indian standards. Thus, in all the cases where the maximum principle stress is greater than the above values, tensile cracks will be developed over the surface. The intensity of cracking increases with the increase in the maximum principle stress values.

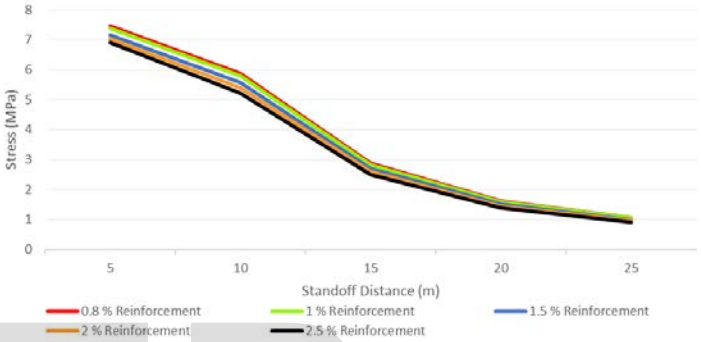

Fig.10. Standoff distance vs Maximum Principle Stress - M 40, 250 kg of TNT and Stirrups at 300 mm

Table.4. Standoff distance vs Maximum Principle Stress - M 40, 250 kg of TNT and Stirrups at 300 mm

Standoff Distance (m)	Maximum Principle Stress (MPa) for reinforcement percentages				
	0.8 %	1 %	1.5 %	2 %	2.5 %
5 m	7.4635	7.3806	7.1718	7.0304	6.9062
10 m	5.8859	5.8019	5.581	5.3952	5.216
15 m	2.8844	2.8369	2.7073	2.5985	2.4883
20 m	1.611	1.583	1.5104	1.4495	1.3879
25 m	1.0705	1.0496	0.9945	0.94979	0.90863

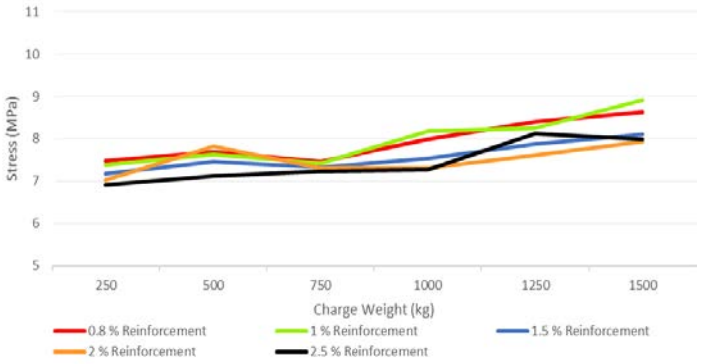

Fig.11. Standoff Distance vs Maximum Principle Stress – M 40, 5 m Blast and No Stirrups

Table.5. Standoff distance vs Maximum Principle Stress - M 40, 5 m blast and No Stirrups

Charge Weight (kg)	Maximum Principle Stress (MPa) for reinforcement percentages				
	0.8 %	1 %	1.5 %	2 %	2.5 %
250 kg	7.478	7.3923	7.1785	7.0313	6.9063
500 kg	7.6919	7.6207	7.455	7.8165	7.114
750 kg	7.4584	7.4176	7.3226	7.3056	7.238
1000 kg	7.9936	8.1692	7.5265	7.3013	7.2701
1250 kg	8.405	8.2495	7.8716	7.6115	8.125
1500 kg	8.6243	8.9125	8.1073	7.9409	7.992

5 Conclusion

The problem of a reinforced concrete pier subjected to blast loading is considered as the core of this thesis. Various cases possible is considered by varying some of the parameters associated with the problem. These various cases were modelled and analyzed. The analysis of the different cases was done using a finite element software package, ANSYS Workbench 17.0 and results were obtained. The results give the deformations and stresses developed for the different cases. Graphs are plotted, compared and the general trends and abnormalities in the graphs are identified, and tried to explain the possible causes for the results in this thesis work.

Considering the percentage of reinforcement in the piers, the deformation created is maximum for piers with 0.8% reinforcement. However, As the standoff distance increases above a particular value, the deformations created is the same for the various reinforcement percentages. Considering the increasing charge weights, the deformations and stresses created in the pier increase with the increase in charge weight for the various percentage reinforcements. But while considering the stresses developed it can be seen that it decreases gradually with increase in the standoff distance, and increases with increase in charge weight. This variation in the behavior of deformations and stresses may be arising due to the lateral and longitudinal stress interactions. For better explanations, further modelling is to be done of piers of different shapes, dimensions and other properties.

The work can further be developed by considering the various parameters that can be changed. Experimental works can also be conducted on scaled or full-sized models to check the analysis results with the actual values. While using scaled models, proper scaling laws must be used before comparing the results.

References

[1] Ghani Razaqpur, Ahmed Tolba, Ettore Contestabile (2016), "Blast Loading Response of Reinforced Concrete Panels Reinforced with Externally Bonded Gfrp Laminates".

[2] M. Remennikov (2003), "A Review of Methods For Predicting Bomb Blast Effects On Buildings", Journal of battlefield technology, Vol 6, no 3. pp 155-161.

[3] A.T.-Blast Version 2.1 (2004), "Anti-Terrorism Blast", Applied Research Associates, Inc.

[4] Aditya Kumar Singh1, Md. Asif Akbari1 and P. Saha (2014), "Behavior of Reinforced Concrete Beams Under Different Kinds of Blast Loading".

[5] Ashish Kumar Tiwary, Aditya Kumar Tiwary and Anil Kumar (2013), "Blast Loading Effects on Steel Columns".

[6] Avinash C. Singhal, Debra Larson, Sanjay Govil and Vikram Karmakar (2011), "Simulation of Blast Pressure on Flexible Panel".

[7] B.M. Luccioni, R.D. Ambrosini and R.F. Danesi (2004), "Analysis of Building Collapse Under Blast Loads".

[8] Baker, W.E. (1973), "Explosions in Air", University of Texas Press, Austin.

[9] Brode H. L., (1955) "Numerical Solution of Spherical Blast Waves", Journal of Applied Physics, American Institute of Physics, New York.

[10] Hrvoje Draganić, Vladimir Sigmund (2012), "Blast Loading on Structures".

[11] K.A. Marchand, F. Alfawakhiri (2015), "Blast and Progressive Collapse", American Institute of Steel Construction.

[12] Kinney G. F., Graham K.J., (1985) "Explosive Shocks in Air", Springer, Berlin.

[13] Mills C. A. (1987) "The Design of Concrete Structures to Resist Explosions and Weapon Effects". Proceedings of the 1st Int. Conference on concrete for hazard protections, Edinburgh, UK.

[14] Mohammed Alias Yusof, Rafika Norhidayu Rosdi, Norazman Mohamad Nor, Ariffin Ismail, Muhammad Azani Yahya, Ng Choy Peng (2014), "Simulation of Reinforced Concrete Blast Wall Subjected to Air Blast Loading".

[15] Newmark N.M., Hansen R.J., (1961) "Design of Blast Resistant Structures", Shock and Vibration Handbook, Vol.3, Eds. Harris & Crede, McGraw-Hill, New York.

[16] Parag Mahajan, Pallavi Pasnur (2014), "Prediction of Blast Loading and Its Impact on Buildings".

[17] Russell P. Burrell, Hassan Aoude, and Murat Saatcioglu (2014), "Response of SFRC Columns Under Blast Loads".

[18] T. Krauthammer (2008), "Modern Protective Structures", Taylor & Francis Group, LLC.

[19] T. Ngo, P. Mendis, A. Gupta and J. Ramsay (2007), "Blast Loading and Blast Effects on Structure", The University of Melbourne, Australia.

[20] TM 5-1300/NAVFAC P-397/AFR 88-22 (1990), "Structures to Resist the Effects of Accidental Explosions", U. S. Departments of the Army, Navy, and Air Force.

[21] Yazan Qasrawi, Pat J. Heffernan and Amir Fam (2015), "Numerical Modeling of Concrete-Filled FRP Tubes' Dynamic Behavior under Blast and Impact Loading".

[22] Zeynep Koccaz, Fatih Sutcu and Necdet Torunbalci (2008), "Architectural and Structural Design for Blast Resistant Buildings".